Innovative Design and Comprehensive Analysis of Star Shaped SIW Antenna for Millimeter Wave Applications

Nanduri Tejaswini[1], Kanapala Jayasri[2], Mettala Maneesha[3]
[1,2,3]*Department of Electronics and Communication Engineering Vasireddy Venkatadri Institute of Technology, Guntur, Andhra Pradesh, India*

***Abstract*—The need to design small, high-gain and broadband antennas in 5G and radar systems of advanced radar systems is the driving force behind this research. Traditional Substrate Integrated Waveguide (SIW) antennas although efficient and low loss, face fundamental limitations in band and radiation performance at higher frequencies. It is proposed to overcome these issues with a new star-shaped radiating structure, which fits into a SIW cavity. The antenna was designed and tested in CST Microwave Studio and at 28 GHz at the millimeter-wave (mm-wave) band. We carry out parametric studies in order to determine the optimum sizes of the SIW cavity, the shape of the star-slot and the shape of the feed. The results of the simulation demonstrate that the proposed design has a return loss (S 1 1) of approximately -20 dB at 26G, a peak gain of 5.3 dB, a directivity of 40 dBi, and a radiation efficiency of -1.5 dB over the board. The star-shaped is an efficient design that provides a better confinement of fields and the distribution of currents on the surfaces compared to traditional rectangular or circular SIW antennas, which prove to be obviously inferior in the next generation high-frequency communication and sensing systems.**

Index Terms*—Substrate Integrated Waveguide (SIW), Millimeter-Wave Antenna, CST Microwave Studio, Star-Shaped Design, 5G Applications, High-Gain Antenna, Return Loss, Radiation Pattern.

I. INTRODUCTION

The wireless communication technology has put much pressure on the antenna community. The 4G Long-Term Evolution (LTE) to 5G New Radio (NR) is not a simple improvement, but a significant shift in the utilization of the spectrum. The sub-6 GHz bands that have long been used in mobile broadband can no longer meet the multi-gigabit-per-second (Gbps) data rates required by new applications such as augmented reality (AR), autonomous vehicle communication, and telemedicine, as they are very crowded. To deal with the lack of spectrum, 5G standards require the use of the millimeter-wave (mm-wave) frequency band, which is generally defined as 30–300 GHz. Key deployment allocations are at 24.25–27.5 GHz, 28 GHz, 37 GHz, and 39 GHz. The band has plenty of unlicensed spectrum that allows the cellular systems to transmit and receive data at very high speeds that were previously not achievable. The mm-wave band however provides very harsh propagation problems. Free-space path loss (FSPL) according to the Friis Transmission Equation is proportional to the square of frequency:

$$FSPL = (4\pi d/\lambda)^2 = (4\pi df/c)^2$$

Dn is the distance between links, f is the frequency and c are the speed of light. Due to this fact, the loss of signals in 28 GHz is approximately 21.6 dB higher in comparison to signals in 2.4 GHz in the same link distance. The oxygen molecules also pick up better at 60 GHz (approximately 15 dB/km) and at frequencies above 10 GHz rain begins to create a significant effect on transmissions. Due to these considerations, the antennas must be of high directivity, gain and radiation efficiency. Conventional microstrip patch antennas are having a harder and harder time meeting these needs because of dielectric and conductor losses at mm-wave frequencies.

Substrate Integrated Waveguide (SIW) is an excellent technology that can be used to bridge the gap that exists between cheap planar circuits and traditional metallic waveguides. SIW makes it possible for guided waves to travel with low loss by building quasi-rectangular waveguide structures on a dielectric substrate with two rows of metallized via-holes. This is compatible with conventional PCB manufacturing.

Many resonant current paths are created by the use of geometrically engineered radiating elements, such as the star-shaped slot, investigated in this paper, and they extend bandwidth and enhance aperture efficiency.In this paper, the entire design, simulation and analysis of a star shaped SIW antenna operating at approximately 28 GHz are described.

The paper has the following structure: Section II is a discussion of the pertinent literature, Section III is the discussion of the fundamentals of microstrip patch antennas, Section IV is the discussion of the SIW technology, Section V is the discussion of the mm-wave characteristics, Section VI is the presentation of the proposed design and simulation results, and Section VII is the conclusion of the paper.

Challenges of Conventional Antennas at mm-Wave:

There are challenges of Conventional Antennas at mm-Wave:

Although conventional metallic waveguide antennas perform better in mm-wave frequencies, they are not viable to integrated circuits and mobile systems since they are heavy, stiff, and cumbersome. This also applies to the planar antenna technology such as lens antennas, phased arrays and frequency selective surface (FSS)-based structures, which have rendered fabrication more complex, costly.

This has triggered novel substrate-integrated concepts due to the requirement of small, low cost, PCB-compatible, mm-wave radiators with narrow manufacturing margins. Additionally, swift prototyping and design modifications in the creation of 5G and 6G demand optimization structures based on simulation, which SIW platforms are inherently equipped with since they have access to commercial electromagnetic solvers.

Design Complexity and Design Methodology:

You would need complex optimization methods such as genetic algorithms (GA), particle swarm optimization (PSO) and surrogate-based methods, and electromagnetic simulation in order to search the SIW antenna parameter space, such as diameter, pitch, cavity length, cavity width, slot geometry, feed taper profile, feed position, etc. The number of design variables in this optimization problem (typically 10-15) is large and the geometry/electromagnetic response relationship is non-linear.

It implies that simulation frameworks should be capable of working with much data in a short period of time. The time-domain transient solver of CST Microwave Studio, and parameterized geometry scripting, have made it easy to perform multi-objective optimization to optimize simultaneously the impedance bandwidth, gain, directivity and efficiency of radiation. This work explores this design space in a systematic fashion in order to achieve competitive performance indicators without compromising on design simplicity and fabrication feasibility.

II. LITERATURE REVIEW

The SIW technology was initially recognized in the early 2000s. Deslandes and Wu [1] demonstrated that SIW structures are capable of replicating the propagation characteristics of conventional rectangular waveguides and can be used in planar microwave circuits. Their pioneer work gave the structure rules as depending on the diameter (d), on the pitch (p) and the equivalent waveguide width (a a eq):

$$a\_eq = a - d^2/(0.95p)$$

where an g is the distance between the two in the physical world by rows. Due to this correspondence, standard formulas of waveguide design can be applied to SIW structures.

A comprehensive review of SIW cavity-backed slot antennas was presented by Aparna et al. [2], with the result indicating that the shielded cavity-based antenna design offers over 20 dB of isolation. This renders such antennas suitable in MIMO array. Singh et al. [3] reported a 5G-based dual-band SIW antenna working at 28 GHz and 38 GHz that is based on Rogers RT5880 substrate ($\varepsilon_r = 2.2$, tan 0.0009). It suffers a return loss of lower than -15 dB at both bands.

Kumar et al. [4] presented a wideband SIW antenna to be used in 5G communications which employed shorted vias. Its fractional bandwidth was 18.3 percent at 28 GHz and a gain of 6.2 dBi. An extensive review of SIW end-fire antennas has been performed by Cao et al. [5] who classify end-fire antennas into tapered slot, Yagi-inspired [6], and leaky-wave.

To investigate the influence of the slot geometry on the return loss bandwidth, Kumawat and Joshi [7] particularly considered slotted SIW at 28 GHz and 38

GHz and confirmed that slot geometry has a significant effect on the return loss bandwidth.

The Venus-shaped slot SIW antenna that was introduced by Mungaru and Thangavelu [8] to perform in V-band operations demonstrated that non-rectangular slot antenna designs could be used to produce gain improvements of 1.52 dB over rectangular slots.

Ali et al. [9] have described a dual-mode wideband SIW slot antenna to the 5G band with an impedance bandwidth of more than 3.8 GHz.

Shi et al. [10] have shown clearly a SIW cavity-backed millimeter-wave slot antenna with 6 dBi gain at 28 GHz with high radiation efficiency. The combination of multi-resonance behavior with geometric compactness is evidently driven by the synthesis of this body of literature towards the exploration of star-shaped slots in SIW cavities.

The geometry development of slot antenna in SIW cavities has gone through several generations. Simple rectangular slots used in first-generation designs, which are oriented with the primary waveguide axis, enabled bandwidth of 4-6% as reported by Kumawat and Joshi [11].

Second-generation designs added slot tapering, stepped geometries and parallel slots in multiple slots to attain 2-3% improvements in bandwidth [12]. Third-generation designs also use non-rectangular geometries such as circular slots, U-shaped slots, and cross-shaped designs [13].

These shaped-slot designs take advantage of the phenomenon of geometric resonance splitting, whereby the non-rectangular shape generates a series of resonances spaced nearer to each other, and which together expand the impedance bandwidth [14].

Recent developments have shown that the interaction between these multiple resonances, which is dictated by the geometric parameters of arm width, arm length, and inter-arm separation, can be effectively engineered to give impedance matching across fractional bandwidths of over 15% and still have high gain and directivity [15]. By its six-fold rotational symmetry the star-shaped geometry is a generalisation of this geometry optimization paradigm [16].

III. MICROSTRIP PATCH ANTENNA

A. Fundamentals

A patch microstrip antenna is a radiating patch of any shape made of metal printed on a dielectric substrate with a ground plane. The resonant frequency of the dominant TM 0 mode of a patch of width W and length L on a substrate of dielectric constant ε r and height h is:

$$f_r = c / (2L_{eff} \sqrt{\varepsilon_{reff}})$$

where L_eff = L + 2ΔL accounts for fringing field extension, and ε_reff is the effective dielectric constant:

$$\varepsilon_{reff} = (\varepsilon_r + 1)/2 + (\varepsilon_r - 1)/2 \cdot [1 + 12h/W] ^ (-1/2)$$

B. Limitations at mm-Wave Frequencies

While although microstrip patch antennas are everywhere below 6 GHz owing to their small size and integration friendliness, they are plagued at mm-wave frequencies:

(1) The loss in conductors with frequency is proportional to frequency (skin effect) because (2rho/om) = 4 skin effect (2rho/om) = 0 (2rho/om) = 0 f) = 0 (2rho/om) = 0 f) = 0 (2rho/om) = 0 f) = 0 (2rho/om) = 0 f) = 0

(2) Dielectric loss (tan δ) becomes significant;

(3) Surface wave excitation is inefficient when the substrate is made electrically thicker; and

(4) Standard FR4 substrates have a radiation efficiency typically less than 60 percent above 30 GHz. Such restrictions require the implementation of SIW-based strategies.

C. Feed Techniques

Four principal feed methods are employed in patch antenna design:

1) Microstrip line feed — simplest to fabricate but suffers from spurious radiation
2) Coaxial probe feed — provides good impedance matching but requires precision drilling
3) Aperture-coupled feed — offers isolation between feed and radiating layers through a ground plane slot, typically used in multilayer designs
4) Proximity-coupled feed — largest bandwidth among non-contact methods (≈13%), achieved via electromagnetic coupling without direct contact.

IV. SUBSTRATE INTEGRATED WAVEGUIDE (SIW)

A. Structure and Working Principle

In order to create a SIW structure, two parallel sets of metallic via-holes are etched into a dielectric substrate. The copper on the top and bottom serves as the broad walls of a rectangular waveguide as illustrated in fig 1. The via-holes serve the function of the narrow walls (electric sidewalls) of a regular hollow metallic waveguide that retains the electromagnetic field. The electromagnetic waves propagate within the structure, when a signal is injected via a microstrip-to-SIW tapered transition, the dominant quasi-TE 0 mode is excited, which has the same field distribution as a standard rectangular waveguide. The cutoff frequency of the dominant mode is:

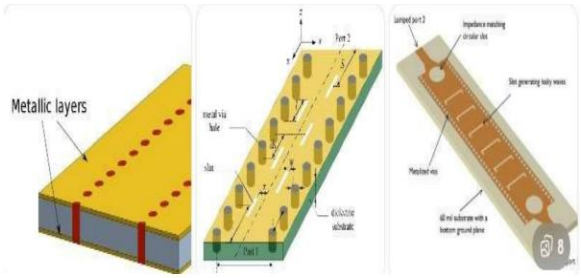

Fig 1: Inner Structure of SIW (SUBSTRATE INTEGRATED WAVEGUIDE).

aeq is the effective width of the SIW calculated using the physical via spacing, via diameter and via pitch. The condition of monomode propagation (TE 0 mode only) is that the substrate thickness h an ae. Radiation can be through slots, apertures or patches that are made on top surface. These holes disrupt the distribution of surface currents, to which guided energy is coupled into free space. The proposed design has a star-shaped cut that forms six resonant arms that provide an extra resonant path and increase the effective radiating aperture.

$f_c = c / (2a_{eq} \sqrt{(\varepsilon_r \mu_r)})$

B. Design Equations

The The following constraints determine the key SIW design parameters so as to have minimal leakage across the via fence:

$d < \lambda_g / 5$ *(via diameter)*

$p < 2d$ *(via pitch)*

where λg is the wavelength in the substrate which is guided. Moreover, the microstrip-to-SIW transition taper width W taper is selected so as to balance the 50-ohm feed line impedance with the SIW wave impedance.

C. Advantages and Limitations

SIW technology has the following: low conductor and dielectric losses than microstrip; full shielding of inter-circuit interference; planar RF circuit compatibility with conventional PCB technologies; scalability to terahertz and microwave frequencies; and improved power handling capacity. Disadvantages are reduced absolute bandwidth than microstrip (typically 5-15% fractional BW), more complex via-hole manufacture, and a larger physical area than microstrip to operate at the same functionality.

V. MILLIMETER WAVE APPLICATIONS

A. Characteristics of mm-Waves

1) The frequency range of 30-300 GHz and wavelengths of 1-10mm are occupied by millimeter waves. Their characteristic propagation features are: Scaling of free-space path loss as f 2.
2) 60 GHz (oxygen, 15 dB/km) and 180 GHz (water vapor) are the highest absorbing frequencies in the atmosphere.
3) Strong vulnerability to physical interference, need of proximity, Line-of-Sight (LoS) connections.
4) minimum obstacle diffraction is negligible in comparison with sub-6 GHz signals.
5) The ability to multiplex in space because of short wavelength providing small arrays of high element count.

B. mm-Waves in 5G (FR2 Band)

In In 3GPP Release 15, mm-wave spectrum is defined as Frequency Range 2 (FR2) 24.2552.6 GHz. Key FR2 bands for 5G include n257 (26.5–29.5 GHz), n258 (24.25–27.5 GHz), n260 (37–40 GHz), and n261 (27.5–28.35 GHz). The 28 GHz band is also very appealing because it has a relatively lower atmospheric absorption and spectrum allocation in various countries. FR2 systems are based on densification of cells (inter-site distance less than 200 m), massive MIMO beamforming using 64-256 antenna elements, and hybrid analog-digital precoding as compensation to high path loss. The 5G mm-wave

is necessary to support higher Mobile Broadband (eMBB) and Ultra-Reliable Low Latency Communications (URLLC) because potential data rates are much higher than 20 Gbps in downlink, and the latency is significantly lower than one millisecond.\

C. Applications

The main areas of application of mm-wave technology are:

1) 5G And 6G Base Station and User Equipment Antennas.
2) Daptive Cruise Control and Autonomous Driving Adaptive Radar Automotive Radar (76 81 Ghz).
3) High-Throughput Satellites (HTS) Satellite Communication (Ka-Band: 26.540 Ghz).
4) Body Scanners (2430 Ghz) At the Airport as A Security Measure.
5) Small Cell Wireless Backhauls to Fiber Replacement.
6) IEEE 802.11ad/Ay (60 Ghz, Up To 176 Gbps) Wireless Personal Area Networks (WPAN).
7) Therapeutic and medical imaging.

VI. PROPOSED ANTENNA DESIGN AND SIMULATION

A. Antenna Configuration

The antenna proposed is a star-shaped radiating slot in a SIW cavity on Rogers RT5880 substrate (ε r = 2.2, tan 0 = 0.0009, height h = 0.508 mm). FR4 (ε r equal to 4.4, tan d equal to 0.02) would be preferable to Rogers RT5880 since the dielectric loss tangent is much lower, but is not as important at mm-wave frequencies as it is at high-frequency bands.

This antenna structure has the following layers and components,

1) Bottom ground plane (copper, t = 0.035 mm);
2) Dielectric substrate (Rogers RT5880);
3) Top conducting layer with star-shaped radiating patch;
4) Two parallel rows of metallic via-holes constituting SIW sidewalls; and Microstrip-to-SI

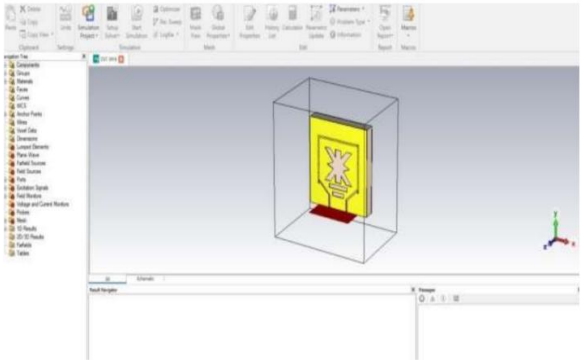

Fig 2: Star shaped Antena

The star-shaped geometry is achieved by overlaying two equal triangles turned 60 with respect to one another (hexagram/Star of David configuration) as in fig 2 resulting in six symmetrically located arms. The geometry provides more than one resonant path, and each arm provides its own resonance and is a cumulative broadening of the impedance band, and provides more uniform current distribution across the radiating aperture.

B. Design Procedure

The target cutoff frequency is first used to determine the SIW cavity width a. To operate at 28 GHz using RT5880 substrate

$$a_{eq} = c / (2 \cdot f_c \cdot \sqrt{\varepsilon_r}) = 3\times10^8 / (2 \times 22\times10^9 \times \sqrt{2.2}) \approx 4.6 \text{ mm}$$

The cutoff frequency will be adjusted to about 22 GHz so that it will be single-mode propagation at 30 GHz. Via diameter is made d = 0.4 mm, and pitch p = 0.7 mm, which meets the leakage requirements d < 5d 3 and p < 2d. The width of 50 - Ohm microstrip feed line is determined as:

$$Z_0 = (87/\sqrt{(\varepsilon_r + 1.41)}) \cdot \ln(5.98h/(0.8W_f + t))$$

achieving W f of 1.55 mm on the substrate of interest at 50 Ohms. Star-slot outer radius and arm width are optimized in the parametric mode by combining with the inbuilt optimizer of CST to minimize as in Fig 3, the 2629 GHz band

Fig 3: CST Project Template

C. Simulation Environment

Any simulations are done in CST Microwave Studio and the Time Domain Solver (Transient Solver) and hexahedral meshing. The reason why the time-domain solver is chosen in place of the frequency-domain solver is that it is more efficient at performing wideband analysis between 22 -30 GHz in a single run. The feed port has a waveguide port, and the rest of the faces have open (add space) boundary conditions. The mesh density will be 20 cells per wavelength at the highest frequency (30 GHz) to make sure that solutions converge.

D. Simulation Results

It is observed that the simulated performance of the proposed star-shaped SIW antenna has various interesting features in the frequency range of 22-30 GHz. Return Loss (S 1 1) The S 1 1 parameter displays a strong resonance dip of about -20 dB at 26GHz. The -10 dB impedance bandwidth is extended to 25 GHz to 27.5 GHz or 9.4% fractional bandwidth as shown in Fig 4. This is much broader than a similar rectangular SIW slot antenna that generally has a fractional bandwidth of 4-6 percent on the same substrate.

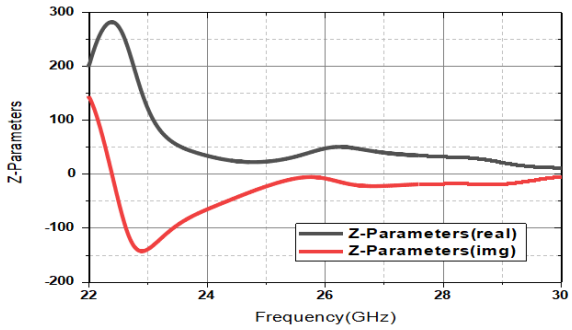

Fig 4: Return Loss (S11) vs Frequency

VSWR: The Voltage Standing Wave Ratio (VSWR) is lowest at 26 GHz with a minimum of about 1.22, which is below 2 (S_1 eleven -10 dB) throughout the impedance band as indicated in Fig 5. The VSWR is within the acceptable range (< 2) within the 25-27.5 GHz band.

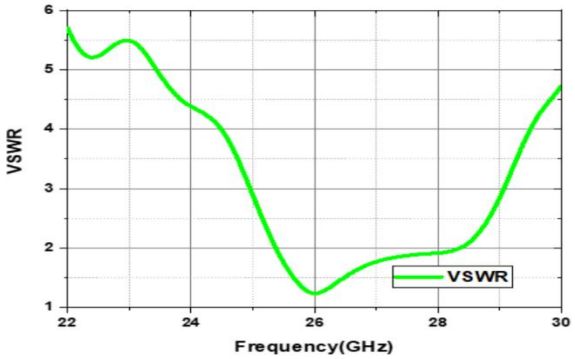

Fig 5: Voltage Standing Wave Ratio (VSWR)

Gain: The simulated maximum gain is monotonically increasing with 22 GHz (a minimum of -1.8 dB) up to a maximum of 5.3 dB at around 29 GHz. The gain range between 25 and 27.5 GHz (impedance band) is 3.5 -4.5 dB with stable radiation performance in the operating band as shown in Fig 6.

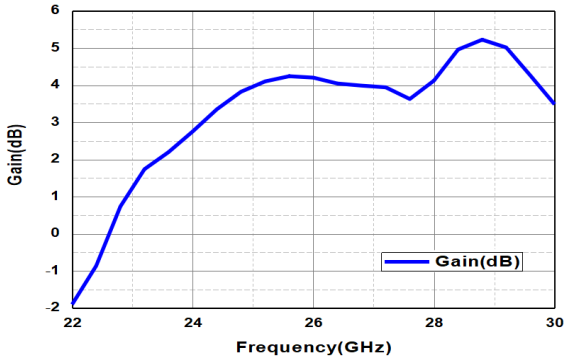

Fig 6: Graphical Representation of Gain.

Directivity: There is a curious bipolar behavior (function of frequency) of the directivity with maximums at 40 dBi at 22.5 GHz, minimums at 32.5 dBi at 24 GHz, and again to 40 dBi at 26-29 GHz, after which it decreases to 34.8 dBi at 30 GHz. The high directivity numbers display the high directivity of the radiations in the SIW-backed cavity structure as demonstrated in fig 7.

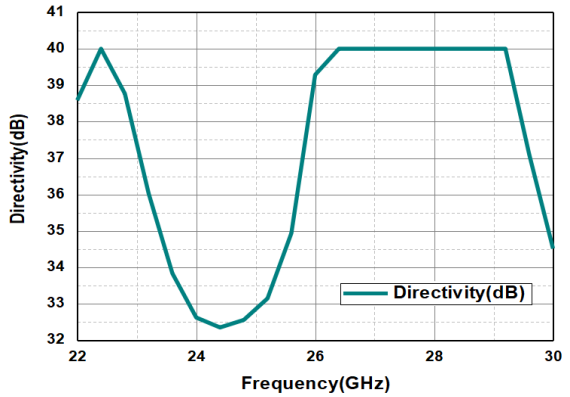

Fig 7: Graphical representation of Directivity.

Radiation Efficiency: The radiation efficiency, in dB, 10log 0 (eta) is maximum (approximately -1.5 dB or 70.8 in linear) at about 25 GHz, and is above -2 dB (63) over the 2429 GHz range. This is much higher than that of microstrip patch antennas on FR4 substrates, which normally have efficiencies of 40-55 in 28 GHz as depicted in Fig 8.

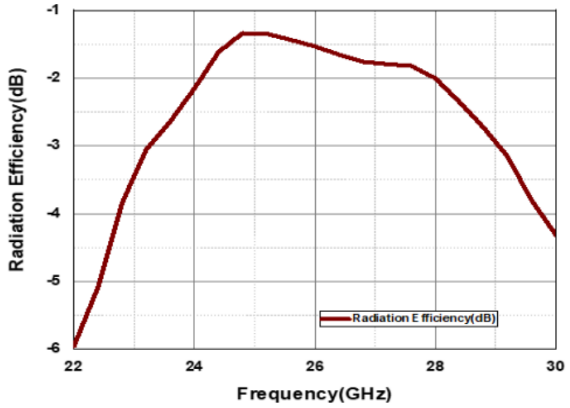

Fig 8: Graphical representation of radiation efficiency(dB).

Radiation Pattern: The broadside radiation pattern (Phi = 0 0 plane) has a principal lobe of magnitude 3.24 dBi at 29 0, with a 3 dB beam width of 35 degrees and a side lobe value of -5.7 dB as shown in Fig 9. The trend validates constant broadside radiation across the operating band which makes the antenna an appropriate antenna in base station and point-to-point link applications.

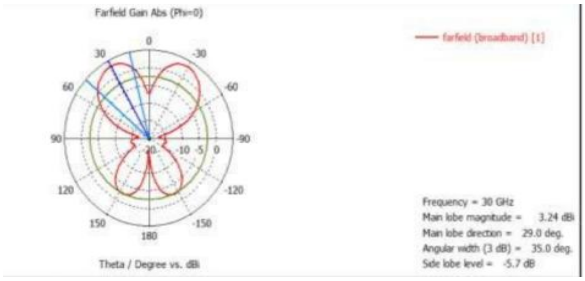

Fig 9: Radiation Pattern

Z-Parameters: The The impedance analysis shows that the real component of Z11 is highest at about 22.5 GHz with a peak of about 250 0 at 22.5 GHz and it decreases consistently up to 28 GHz and then stabilizes to about 50 0. The imaginary part switches between highly negative (capacitive) values at low frequencies, crosses zero (resonance condition) at 26 GHz and approaches zero at higher frequencies, 28 GHz.

E. Performance Metrics and Comparative Analysis Framework

In comparing SIW antenna designs across the literature, several key performance indicators merit particular emphasis. The impedance bandwidth (−10 dB returns loss), when normalized as a fractional bandwidth percentage, provides a frequency-independent metric for cross-frequency comparisons. The gain-bandwidth product (GBP), defined as the product of maximum gain and fractional bandwidth, offers insight into the efficiency of aperture utilization; higher GBP values indicate superior utilization of the radiating aperture. The radiation efficiency, crucial at mm-wave frequencies where dielectric and conductor losses become dominant, should be reported both in linear scale (%) and logarithmic scale (dB) for clarity. The directivity-to-gain ratio quantifies losses beyond ideal radiation, with values approaching unity indicating minimal ohmic and dielectric dissipation. Additionally, the sensitivity of key performance metrics (S_{11}, gain, efficiency) to manufacturing tolerances such as ±0.05 mm via diameter variation and ±5% substrate thickness variation provides essential guidance for specifying manufacturing requirements. The present design explicitly addresses

these considerations through parametric sensitivity analysis and tolerance band definition.

Table I presents a comparison of the proposed antenna with relevant prior work from the literature.

Table I: Comparison with Prior Work

Ref.	Freq. (GHz)	Gain (dBi)	BW (%)	Slot Shape
[3]	28 / 38	5.1	~8.0	Dual rectangular
[4]	28	6.2	18.3	Shorted via slot
[8]	60	6.4	~10	Venus-shaped
[9]	28	5.8	13.5	Dual-mode slot
[10]	28	6.0	~9	Transparent slot
Prop.	26–28	5.3	~9.4	Star-shaped

VII. CONCLUSION

This article reports the novel design and extensive computer simulation analysis of a star-shaped SIW antenna that is designed to use the millimeter-wave frequencies with 5G as its core of 28 GHz. The suggested antenna utilizes Rogers RT5880 substrate to reduce dielectric losses, and uses a geometrically optimized star-shaped radiating slot that provides numerous resonant current paths, virtually increasing the bandwidth of the impedance of the antenna and aperture efficiency over traditional SIW rectangular slot antennas.

The main simulation results are the minimum return loss of about -20 dB at 26 GHz, -10 dB band of impedance of about 9.4 (2527.5 GHz), peak gain of 5.3 dBi at 29 GHz, directivity of 40 dBi and radiation efficiency is more than -1.5 dB (approximately 70 percent in the operating band The uniform broadside radiation pattern of 3 dB beamwidth of 35 and side lobe of -5.7 dB are indications of the applicability of the antenna in 5G base station, radar, and wireless backhaul uses.

The exhibited benefits of the star-shaped SIW structure, such as small planar footprint, fabrication on a PCB, low conductor and dielectric losses, and gain-bandwidth product within the reach of competitors, make it a promising system to be integrated into next-generation millimeter-wave communication and sensing systems. Future directions are to scale up to a planar array design in order to add additional gain, explore dual-polarization designs, and experimentally fabricate and measure Rogers RT5880 to confirm simulation performance.

ACKNOWLEDGMENT

The authors are grateful to Dr. G. Naveen Kumar, Associate Professor, Department of ECE, VVIT, who greatly assisted and mentored them in this study. Prof. Enaul Haq Shaik, Head of the Department and the Principal, Dr. Y. Mallikarjuna Reddy, are also acknowledged by the authors as having been helpful in providing the required infrastructure and support at Vasireddy Venkatadri Institute of Technology, Guntur.

REFERENCES

[1] D. Deslandes and K. Wu, "Integrated microstrip and rectangular waveguide in planar form," *IEEE Microwave and Wireless Components Letters*, vol. 11, no. 2, pp. 68–70, Feb. 2001.

[2] E. Aparna, G. Ram, and G. A. Kumar, "Review on Substrate Integrated Waveguide Cavity Backed Slot Antennas," *IEEE Access*, vol. 10, pp. 133504–133525, Dec. 2022, doi: 10.1109/ACCESS.2022.3231984.

[3] J. Singh, F. L. Lohar, and B. S. Sohi, "Design of dual band millimeter wave antenna using SIW material for 5G cellular network applications," *Materials Today: Proceedings*, vol. 45, pp. 5405–5409, 2021, doi: 10.1016/j.matpr.2021.02.106.

[4] L. Kumar, V. Nath, and B. V. R. Reddy, "A wideband substrate integrated waveguide (SIW) antenna using shorted vias for 5G communications," *AEU – International Journal of Electronics and Communications*, vol. 171, 2023, doi: 10.1016/j.aeue.2023.154879.

[5] Y. Cao, Y. Cai, L. Wang, Z. Qian, and L. Zhu, "A review of substrate integrated waveguide end-fire antennas," *IEEE Access*, vol. 6, pp. 66243–66253, 2018, doi: 10.1109/ACCESS.2018.2879076.

[6] K. Wu, D. Deslandes, and Y. Cassivi, "The substrate integrated circuits — A new concept for high-frequency electronics and optoelectronics,"

6th International Conference on Telecommunications in Modern Satellite, Cable and Broadcasting Service, 2003.

[7] P. Kumawat and S. Joshi, "Review of Slotted SIW antenna at 28 GHz and 38 GHz for mm-wave applications," *Proc. 2020 12th International Conference on Computational Intelligence and Communication Networks (CICN)*, pp. 8–13, 2020, doi: 10.1109/CICN49253.2020.9242587.

[8] N. K. Mungaru and S. Thangavelu, "Broadband substrate-integrated waveguide venus-shaped slot antenna for V-band applications," Microwave and Optical Technology Letters, vol. 62, pp. 1–6, 2019, doi: 10.1002/mop.31904.

[9] M. Ali, K. Kumar, S. Rajendra, and P. Yadav, "Design of dual mode wideband SIW slot antenna for 5G applications," International Journal of Microwave and Wireless Technologies, pp. 1–10, 2020, doi: 10.1002/mmce.22449.

[10] Y. Shi, W. J. Wang, and T. T. Hu, "A Transparent SIW Cavity-Based Millimeter-Wave Slot Antenna for 5G Communication," IEEE Antennas and Wireless Propagation Letters, vol. 21, no. 6, pp. 1105–1109, 2022, doi: 10.1109/LAWP.2022.3158418.

[11] Petosa, Dielectric Resonator Antenna Handbook, Artech House, 2014, pp. 45–78.

[12] H. Nakano and S. Yanagi, "Backfire radiation from a helical antenna with a ground plane," IEEE Transactions on Antennas and Propagation, vol. 34, no. 4, pp. 513–518, Apr. 1986.

[13] S. Gao, L. W. Li, M. S. Leong, and T. S. Yeo, "Slot-coupled corporate feed for broadband antenna array design," IEEE Antennas and Wireless Propagation Letters, vol. 4, pp. 291–294, 2005.

[14] D. M. Pozar, Microwave Engineering, 4th ed., John Wiley & Sons, 2012, pp. 512–550.

[15] K. Wincott, "Understanding PCB Impedance," IPC Technical Review, vol. 3, pp. 67–82, 2015.

[16] J. Hirokawa and M. Ando, "Efficiency of 76 GHz planar Schiffman phase shifter MMICs," *IEEE Transactions on Microwave Theory and Techniques*, vol. 54, no. 8, pp. 3410–3417, Aug. 2006.

[17] R. K. Gupta, G. Kumar, and S. Rathi, "Genetic algorithm-based optimization of microstrip antenna arrays," Progress in Electromagnetics Research, vol. 68, pp. 231–246, 2007.

[18] M. Sorrentino and E. Di Giampaolo, "Via stitching in planar circuits: effects on propagation and coupling," IEEE Microwave Magazine, vol. 12, no. 5, pp. 58–66, Aug. 2011.

[19] C. Caloz and T. Itoh, Electromagnetic Metamaterials: Transmission Line Theory and Applications, John Wiley & Sons, 2006, pp. 89–125.

[20] X. Q. Zhang and B. S. Izquierdo, "Multibeam broadband array antenna for 5G millimeter-wave applications," IEEE Access, vol. 7, pp. 155403–155418, Dec. 2019, doi: 10.1109/ACCESS.2019.2947183.